Local Diffusion Map Signature for Symmetry-aware Non-rigid Shape Correspondence

Meng Wang
NYU Multimedia and Visual Computing Lab
Dept. of ECE, NYU Abu Dhabi, UAE
Dept. of CSE, NYU Tandon School of Engineering, USA

Yi Fang*
NYU Multimedia and Visual Computing Lab
Dept. of ECE, NYU Abu Dhabi, UAE
Dept. of ECE, NYU Tandon School of Engineering, USA

ABSTRACT

Identifying accurate correspondences information among different shapes is of great importance in shape analysis such as shape registration, segmentation and retrieval. This paper aims to develop a paradigm to address the challenging issues posed by shape structural variation and symmetry ambiguity. Specifically, the proposed research developed a novel shape signature based on local diffusion map on 3D surface, which is used to identify the shape correspondence through graph matching process. The developed shape signature, named local diffusion map signature (LDMS), is obtained by projecting heat diffusion distribution on 3D surface into 2D images along the surface normal direction with orientation determined by gradients of heat diffusion field. The local diffusion map signature is able to capture the concise geometric essence that is deformation-insensitive and symmetry-aware. Experimental results on 3D shape correspondence demonstrate the superior performance of our proposed method over other state-of-the-art techniques in identifying correspondences for non-rigid shapes with symmetry ambiguity.

Keywords

3D shape correspondence; non-rigid shape matching; 3D shape signature

1. INTRODUCTION

1.1 Background

Shape correspondence provides important information for many shape analysis such as shape alignment and registration, texture mapping, information transformation among shapes, shape morphing, statistical shape modelling and so on. It is therefore of great interest to develop the efficient

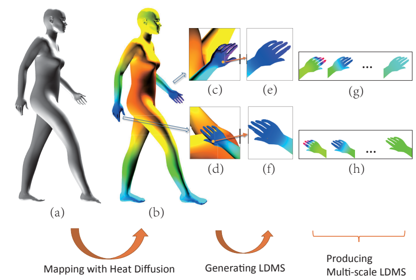

Figure 1: Pipeline of our method.

shape correspondence algorithm that, given a pair of shapes, return the corresponding regions on surface. The accuracy of shape correspondence algorithm is ultimately determined by the quality and characteristics of the shape signature that captures the geometric essence of points on 3D surface. While many advancements have been made for shape correspondence over the years, there remain challenges in the development of effective and discriminative shape signature. Two such challenges are shape structural variations and symmetry ambiguity and both can significantly degrade the performance of a shape correspondence technique[13, 12, 7, 18]. Therefore, a robust shape signature should be able to address the following issues.

- Structural variation in 3D models.
- Symmetry ambiguity in 3D shapes.
- Noise and incompleteness present in 3D shape description.

1.2 Related Work

3D non-rigid shape correspondence has been received considerable attention from computer vision and graphics areas. Many 3D objects contain dynamical units with their 3D shape flexibility and variations play an essential role in certain types of functional processes. The non-rigid shape correspondence methods often attempt to find correspondence information through a feature matching process. The process starts with computing a certain type of shape signature that capture geometric characteristics for representative

*Corresponding author. Email: yfang@nyu.edu

MM '16, October 15-19, 2016, Amsterdam, Netherlands

DOI: http://dx.doi.org/10.1145/2964284.2967277

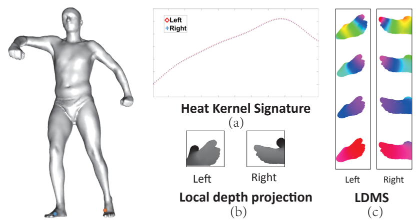

Figure 2: Local descriptor comparison between HKS(middle up), local depth descriptor(middle bottom) and multi-scale HKS projection descriptor(right). HKS cannot separate left and right foot, local depth projection is not discriminative, multi-scale HKS projection is discriminative between left and right foot.

points sampled on shape surface, then identifies a sparse correspondence by solving an assignment problem which maximize the similarity between the set of shape signatures with a certain type of spatial constrains such as preservation of geometric distance among corresponding pairs[17, 16]. Since a complete survey of non-rigid shape correspondence techniques is beyond the scope of this research paper, we refer the interested readers to review papers [17] for a comprehensive summary of the detailed techniques. As we can see from the feature matching process, the non-rigid shape correspondence can essentially boils down to two key components: the shape signature and assignment algorithm. Given an assignment algorithm, the accuracy of shape correspondence algorithm is ultimately determined by the quality and characteristics of the shape signature.

There have been a significant works on shape signatures in computer graphics community. [15, 3] Although those shape signatures are able to robustly capture the deformation invariant feature, all of them face with the symmetry ambiguity challenge. Early attempt to address the symmetry ambiguity takes advantage of the distortion measures based on conformal mapping[8, 10] or symmetry information[12]. However, these methods are restricted to meshes with same genus and require the mesh to be quite close to each other. Most recently, Yoshiyasu presented an orientation-aware local shape descriptors that be used for finding correspondence for shapes present incompleteness and symmetry [18].

1.3 Our shape signature: Local Diffusion Map Signature

Based on the diffusion geometry, we proposed a local diffusion map signature (LDMS) based on a novel strategy of projecting heat diffusion distribution on 3D surface into 2D image along the direction determined by gradients of heat diffusion field. Figure 1 illustrates the pipeline of generating LDMS, which mainly includes three steps. The first step is mapping a 3D surface with heat diffusion distribution. A variety of heat diffusion distribution, such as HKS, SIHKS, and Heat Kernel Matrix, can be chosen for this purpose. HKS is chosen in our development. The Figure 1(b) is a mapping of HKS on 3D surface shown on Figure 1(a). And Figure 1(c) and Figure 1(d) are closeup view of left and right hand region for human model. The second step is generating LDMS for repressive points sampled from 3D shape. The Figure 1(e) and Figure 1(f) illustrate the LDMS for points sampled from left and right hand respectively. The third step is producing a multi-scale LDMS for repressive points sampled from 3D shape. The multi-scale LDMS is produced by concatenating 2D images by projecting HKS based heat diffusion distribution at different scales. As we can see from Figure 2, the HKS (Figure 2(a))for sampled points from left and right hand are almost identical, whereas the local depth projection (Figure 2(b)) and LDMS (Figure 2(c)) can differentiate those points. In addition, multi-scale LDMS shown in Figure 2(c) provides much more discriminative power compared to local depth projection (shown in Figure 2(b)).

2. METHOD

2.1 Heat diffusion and heat kernel signature

Heat kernel signature[15], which is developed based heat diffusion, has been widely used for 3D shape processing [15]. Heat kernel signature is defined by:

$$HKS(x) = (h_{t_1}(x, x), h_{t_2}(x, x), \ldots, h_{t_n}(x, x)) \quad (1)$$

where x denotes a point on the surface, $HKS(x)$ denotes the heat kernel signature at point x, $h_t(x, x)$ denotes the heat kernel value at point x, t_n denotes the nth sample point in time. A number of attractive attributes, including invariance to isometric transformation, robustness to noise, and multi-scale representation, make HKS a popular signature in community[15]. Our LDMS is developed based on HKS as described below.

2.2 Local diffusion map signature (LDMS)

LDMS is proposed primarily to address two challenging shape correspondence issues: structural variations and symmetry ambiguity. As shown in Figure 1, there are three main steps in producing a LDMS and multi-scale LDMS for a sampled point on 3D surface. Subsections below, which include representative points sampling, local diffusion map, stable orientation direction, and generation of LDMS, provide with detailed descriptions for LDMS computation.

Representative points sampling: A triangulated 3D mesh normally contains a large number of vertex on its surface. It is therefore very time-consuming and computationally inefficient for a shape correspondence algorithm considering all of the vertex to establish a dense correspondence between a pair of shapes. In our work, DoG detector [4] is used to identify the representative samples on surface and a density-invariant smoothing strategy [4] is employed to reduce the influence due to the sampling density. With result of correspondence of sampled points, a dense shape correspondence can be established by various approaches like [14].

Local diffusion map: In this paper, we define local diffusion map as a regional heat diffusion distribution of HKS values for a specific point at a time scale. For each point on the surface (for example, a sampled point on right hand as shown in Figure 1(d)), a local diffusion map reflects two important information 1)the HKS values for its neighbour points, 2) the spatial orientation of its neighbour points. As described in [15], HKS capture intrinsic geometric feature for points on surface. However, it loses the spatial orientation information. This explains why HKS values for points sampled from left and right hands are almost identical as shown in Figure 2(a). Therefore, to capture symmetry-aware information, we need to further exploit the spatial orientation

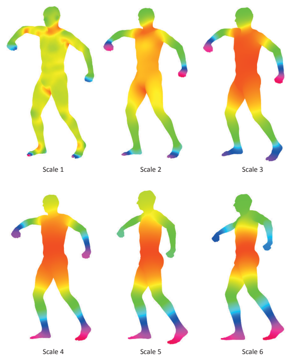

Figure 3: Diffusion map on a 3D surface at different scales.

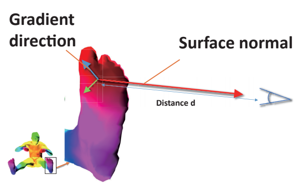

Figure 4: Demonstration of projecting a local diffusion map to 2D image.

information contained in local diffusion map. In this paper, we developed a method of determining a stable orientation from gradients of heat diffusion field, which is explained in the following subsection. Note that local diffusion map also has multi-scale property due to the multi-scale nature of HKS. Figure 3 illustrate the diffusion map for the entire 3D surface at six different scales.

Stable orientation direction: Previous work [4] suggests the principle component vector based PCA analysis is able to provide a reasonable orientation direction for a surface point. However, this direction is not stable especially for points on the surface of non-rigid shapes with the local deformations. In [18], the authors suggest that the gradients of average diffusion distance field will give a more stable orientation direction compared to the principle component vector. In this paper, we develop a way to determine the orientation from gradients of heat diffusion field which is computed by averaging diffusion maps at all scales. Although the determination of orientation direction is similar to the approaches in [4, 18], our experimental experience indicates that our orientation direction is more stable probably due to multi-scale nature of diffusion map.

Generation of LDMS: The newly proposed LDMS is generated by projecting local diffusion map into 2D image. To perform a projection from a local diffusion map on 3D surface to a 2D image, we require to have three critical parameters to set up a camera: camera position, viewing direction and camera rotation (up direction). As shown in Figure 4, the viewing direction is the opposite direction of surface normal, the camera is placed at some position on the normal direction line with a distance of d to the surface point, and the camera rotation is set as the stable orientation direction determined in subsection above. The LDMS for a surface point is generated by projecting a local diffusion map to a 2D image based on the camera setting. In addition, the multi-scale property of the local diffusion map can naturally give rise to a multi-scale nature for LDMS by projecting multi-scale local diffusion map as shown in Figure 1(g). The multi-scale LDMS is able to boost the discriminative power of the shape signature.

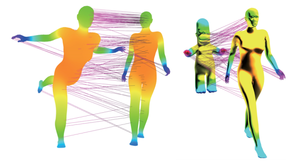

Figure 5: Shape correspondence over nonrigid models

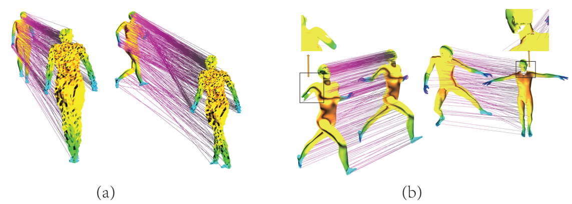

Figure 6: Shape correspondence over noise models and partial models

3. EXPERIMENT

We carry out a set of experiments for finding shape correspondence and assessed the performance of our LDMS. The 3D models were chosen from the following databases: SCAPE [5], TOSCA [2], and Watertight [6] database. The SCAPE library has 71 human meshes in total, which is 3D human surface library with realistic muscle deformation in different poses. The 3D models from datasets have undergone different types of geometric transformations which lead to various levels of structural variations. Models in Figure 5, 6 are from TOSCA [2] and Watertight [6] database.

In the experiments, all the shapes are resampled to have approximately the same amount of faces. The represented sample points are selected by the DoG detector or by consistent selection from ground truth correspondence. For the heat diffusions we sampled 101 scales in time interval of 0.0065. For each sample point, we generate six LDMS by choosing local diffusion map at six different time scales (1,21,41,61,81,101). We normalized the shape coordinates to $1/max(max(\mathbf{X}-average(X)), max(\mathbf{Y}-aver(Y)), max(\mathbf{Z}-aver(Z)))$ of original magnitude, where $\mathbf{X}, \mathbf{Y}, \mathbf{Z}$ are physical coordinates of all the input points. Each LDMS has a resolution of 50 pixel $\times$ 50 pixel.

3.1 Shape correspondence for non-rigid models

In this experiment, we test the performance of LDMS for finding correspondence on nonrigid shape models. We carry out two sets of tests using 3D models present in different types of nonrigid deformation. In the first test, we aim to establish the shape correspondence between 3D models with articulated deformation. We selected a pair of 3D human models at different poses as shown on the left side of Figure 5. In the second test, we aim to identify the shape correspondence between 3D models with non-isometric deformation, which is generally considered as much more challenging deformation for a shape correspondence method. We chosen a 3D human model and a 3D homer model as shown on the right side of Figure 5. All of the 3D models selected in this experiment are present in symmetry. The shape correspondence results can be found in Figure 5, where the red lines link the corresponding points between two models. The accurate correspondence shown in Figure 5 indicates that our LDMS captures deformation-insensitive and symmetry-aware geometric essence.

3.2 Shape correspondence for noise models

In this experiment, we will demonstrate that LDMS is robust to numerical noise. To prepare the noisy model, we simulate noise on the 3D model by randomly perturbing the vertices of original models. As we can see from the Figure 6(a), there are a original model is a 3D human model without noise and a noisy models generated from the original model at a moderate noise level. We can see that the geometric features of the noisy human model have significantly altered and deteriorated. As indicated by the results in Figure 6(a), our method performs very well in identifying correspondence between models with moderate level of noise suggested by the accurate corresponding pair of points linked by red lines in the Figure.

3.3 Shape correspondence for incomplete models

In this experiment, we will design the test that validate the performance of LDMS under the context of incomplete models. To prepare the incomplete 3D models, we select clean models from TOSCA dataset and manually remove some parts from the clean models as shown in Figure 6(b). The figure on left in Figure 6(b) illustrates a pair of 3D human models with one model missing the right arm part. The figure on right in Figure 6(b) displays a pair of 3D human models with one model having a hole on the neck. The close-up figures provide a better view of the incompleteness in original models. As indicated by the results in Figure 6(b), our method works very well for finding the shape correspondence as demonstrated by the accurate corresponding pair of points linked by red lines in the figure.

Methods	Average Geodesic Error
LDMS	**0.039**
Blended	0.081
Mobius Voting	0.162
Best Conformal	0.113
GMDS	0.276
HKM 1 corr	0.272
HKM 2 corr	0.256

Table 1: Result average geodesic error on SCAPE library. 100 uniform vertices are sampled.

3.4 Comparisons with state-of-the-art signatures

In this section, we will conduct an experiment to compare the performance of LDMS to those of other state-of-the-art shape signature. We compared the proposed method with other methods including Blended Intrinsic Maps [8], Mobius Voting [10], GMDS [1] and heat kernel map matching [11] in the benchmark and the most recent SAM method published in CVPR 2014 [18]. The geodesic distortion is defined as the a distance shift from the identified corresponding point to the true one. We provide two quantitative evaluation based on geodesic distortion: 1) Average geodesic error, 2) Geodesic error vs Percentage of corresponding points Curve (GP-curve). The average error measures the overall performance of a shape correspondence based on the mean geodesic errors produced by all corresponding points. As we can see in Table 1, LDMS gives the best correspondence performance as indicated the smallest average geodesic error. The GP-curve evaluates the performance of a shape correspondence at a given level of geodesic error. For each level of geodesic error, GP-curve provides with a percentage of corresponding points that have a lower geodesic error than the given one. In Figure 7, we plot all GP-curves for five different methods. As we can see from the figure, LDMS consistently gives the best performance at all levels of geodesic errors as indicated by the fact that red GP-curve consistently stays on the top of all other GP-curves. The results quantitatively validate the superior performance of our proposed method over other state-of-the-art techniques in identifying correspondences for non-rigid shapes with symmetry ambiguity.

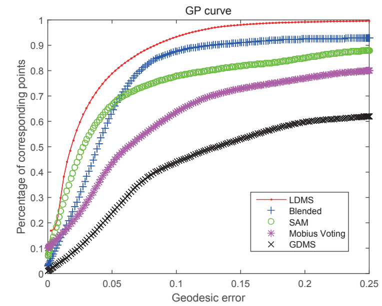

Figure 7: Geodesic error for shape correspondence on SCAPE. 100 uniform vertices are sampled.

4. CONCLUSION

Identifying accurate correspondence information among shapes is of great importance in shape analysis such as shape registration, segmentation and retrieval. In this paper, we proposed a shape signature, named local diffusion map signature (LDMS), that capture the deformation-insensitive and symmetry-aware geometric essence. Driven by LDMS, a shape correspondence paradigm is developed to address the challenging issues posed by shape structural variations and symmetry ambiguity. Experimental results on 3D shape correspondence demonstrate the superior performance of our proposed method over other state-of-the-art techniques in identifying correspondences for non-rigid shapes with symmetry ambiguity.

5. ACKNOWLEDGMENTS

This material is partly based upon work supported by New York University Abu Dhabi institute (AD131 and REF131).

6. REFERENCES

[1] A. M. Bronstein, M. M. Bronstein, and R. Kimmel. Generalized multidimensional scaling: a framework for isometry-invariant partial surface matching. *Proceedings of the National Academy of Sciences of the United States of America*, 103(5):1168–1172, 2006.

[2] A. M. Bronstein, M. M. Bronstein, and R. Kimmel. *Numerical geometry of non-rigid shapes*. Springer Science & Business Media, 2008.

[3] A. M. Bronstein, M. M. Bronstein, R. Kimmel, M. Mahmoudi, and G. Sapiro. A gromov-hausdorff framework with diffusion geometry for topologically-robust non-rigid shape matching. *Int. J. Comput. Vision*, 89:266–286, 2010.

[4] T. Darom and Y. Keller. Scale-invariant features for 3-d mesh models. *Image Processing, IEEE Transactions on*, 21(5):2758–2769, 2012.

[5] P. S. Dragomir Anguelov, H.-C. Pang, D. Koller, and J. D. Sebastian Thrun. The correlated correspondence algorithm for unsupervised registration of nonrigid surfaces. In *Advances in Neural Information Processing Systems 17: Proceedings of the 2004 Conference*, volume 17, page 33. MIT Press, 2005.

[6] D. Giorgi, S. Biasotti, and L. Paraboschi. Shrec: shape retrieval contest: Watertight models track. *Online]: http://watertight. ge. imati. cnr. it*, 2007.

[7] Q.-X. Huang, B. Adams, M. Wicke, and L. J. Guibas. Non-rigid registration under isometric deformations. In *Computer Graphics Forum*, volume 27, pages 1449–1457. Wiley Online Library, 2008.

[8] V. G. Kim, Y. Lipman, and T. Funkhouser. Blended intrinsic maps. In *ACM Transactions on Graphics (TOG)*, volume 30, page 79. ACM, 2011.

[9] C. Li and A. B. Hamza. Spatially aggregating spectral descriptors for nonrigid 3d shape retrieval: a comparative survey. *Multimedia Systems*, 20(3):253–281, 2014.

[10] Y. Lipman and T. Funkhouser. Möbius voting for surface correspondence. In *ACM Transactions on Graphics (TOG)*, volume 28, page 72. ACM, 2009.

[11] M. Ovsjanikov, Q. Mérigot, F. Mémoli, and L. Guibas. One point isometric matching with the heat kernel. In *Computer Graphics Forum*, volume 29, pages 1555–1564. Wiley Online Library, 2010.

[12] M. Ovsjanikov, Q. Mérigot, V. Pătrăucean, and L. Guibas. Shape matching via quotient spaces. In *Computer Graphics Forum*, volume 32, pages 1–11. Wiley Online Library, 2013.

[13] Y. Sahillioğlu and Y. Yemez. Coarse-to-fine isometric shape correspondence by tracking symmetric flips. In *Computer Graphics Forum*, volume 32, pages 177–189. Wiley Online Library, 2013.

[14] A. Sharma, R. Horaud, J. Cech, and E. Boyer. Topologically-robust 3d shape matching based on diffusion geometry and seed growing. In *Computer Vision and Pattern Recognition (CVPR), 2011 IEEE Conference on*, pages 2481–2488. IEEE, 2011.

[15] J. Sun, M. Ovsjanikov, and L. Guibas. A concise and provably informative multi-scale signature based on heat diffusion. *SGP '09: Proceedings of the Symposium on Geometry Processing*, pages 1383–1392, 2009.

[16] A. Tevs, M. Bokeloh, M. Wand, A. Schilling, and H.-P. Seidel. Isometric registration of ambiguous and partial data. In *Computer Vision and Pattern Recognition, 2009. CVPR 2009. IEEE Conference on*, pages 1185–1192. IEEE, 2009.

[17] O. van Kaick, H. Zhang, G. Hamarneh, and D. Cohen-Or. A survey on shape correspondence. *Computer Graphics Forum*, 30(6):1681–1707, 2011.

[18] Y. Yoshiyasu, E. Yoshida, K. Yokoi, and R. Sagawa. Symmetry-aware nonrigid matching of incomplete 3d surfaces. In *Computer Vision and Pattern Recognition (CVPR), 2014 IEEE Conference on*, pages 4193–4200. IEEE, 2014.